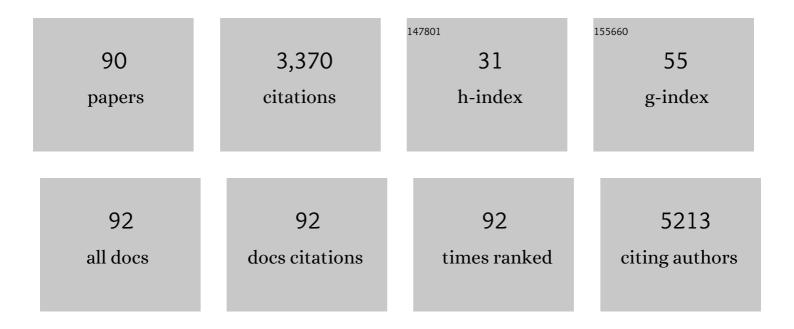
List of Publications by Year in descending order

Source: https://exaly.com/author-pdf/7492946/publications.pdf Version: 2024-02-01



#	Article	IF	CITATIONS
1	Efficient hot-electron transfer by a plasmon-induced interfacial charge-transfer transition. Science, 2015, 349, 632-635.	12.6	951
2	A stable electron-deficient metal–organic framework for colorimetric and luminescence sensing of phenols and anilines. Journal of Materials Chemistry A, 2018, 6, 9236-9244.	10.3	127
3	Increasing Effectiveness of Photogenerated Carriers by in Situ Anchoring of Cu <sub>2</sub> O Nanoparticles on a Nitrogen-Doped Porous Carbon Yolk–Shell Cuboctahedral Framework. ACS Catalysis, 2018, 8, 3348-3356.	11.2	112
4	Universal Length Dependence of Rod-to-Seed Exciton Localization Efficiency in Type I and Quasi-Type II CdSe@CdS Nanorods. ACS Nano, 2015, 9, 4591-4599.	14.6	92
5	Versatile and Switchable Responsive Properties of a Lanthanideâ€Viologen Metal–Organic Framework. Small, 2019, 15, e1803468.	10.0	88
6	Interfacial Clustering-Triggered Fluorescence–Phosphorescence Dual Solvoluminescence of Metal Nanoclusters. Journal of Physical Chemistry Letters, 2017, 8, 3980-3985.	4.6	79
7	Switchable organoplatinum metallacycles with high quantum yields and tunable fluorescence wavelengths. Nature Communications, 2019, 10, 4285.	12.8	73
8	Comprehensive understanding of heat-induced degradation of triple-cation mixed halide perovskite for a robust solar cell. Nano Energy, 2018, 54, 218-226.	16.0	72
9	Extremely Low-Cost and Green Cellulose Passivating Perovskites for Stable and High-Performance Solar Cells. ACS Applied Materials & amp; Interfaces, 2019, 11, 13491-13498.	8.0	71
10	Size-Independent Exciton Localization Efficiency in Colloidal CdSe/CdS Core/Crown Nanosheet Type-I Heterostructures. ACS Nano, 2016, 10, 3843-3851.	14.6	70
11	Engineering an N-doped TiO <sub>2</sub> @N-doped C butterfly-like nanostructure with long-lived photo-generated carriers for efficient photocatalytic selective amine oxidation. Journal of Materials Chemistry A, 2018, 6, 2091-2099.	10.3	67
12	A novel ternary heterostructure with dramatic SERS activity for evaluation of PD-L1 expression at the single-cell level. Science Advances, 2018, 4, eaau3494.	10.3	63
13	Highly Sensitive Hill-Type Small-Molecule pH Probe That Recognizes the Reversed pH Gradient of Cancer Cells. Analytical Chemistry, 2018, 90, 5803-5809.	6.5	56
14	Base Stacking in Adenosine Dimers Revealed by Femtosecond Transient Absorption Spectroscopy. Journal of the American Chemical Society, 2014, 136, 6362-6372.	13.7	54
15	Ultrafast Photoinduced Interfacial Proton Coupled Electron Transfer from CdSe Quantum Dots to 4,4′-Bipyridine. Journal of the American Chemical Society, 2016, 138, 884-892.	13.7	52
16	Quasi-type II CuInS <sub>2</sub> /CdS core/shell quantum dots. Chemical Science, 2016, 7, 1238-1244.	7.4	49
17	Excited States in DNA Strands Investigated by Ultrafast Laser Spectroscopy. Topics in Current Chemistry, 2014, 356, 39-87.	4.0	47
18	Ultrafast nonradiative decay by hypoxanthine and several methylxanthines in aqueous and acetonitrile solution. Physical Chemistry Chemical Physics, 2012, 14, 10677.	2.8	46

JINQUAN CHEN

#	Article	IF	CITATIONS
19	Engineering the Chargeâ€Transfer State to Facilitate Spin–Orbit Charge Transfer Intersystem Crossing in Spirobis[anthracene]diones. Angewandte Chemie - International Edition, 2020, 59, 22179-22184.	13.8	44
20	Hydrogen Bond Donors Accelerate Vibrational Cooling of Hot Purine Derivatives in Heavy Water. Journal of Physical Chemistry A, 2013, 117, 6771-6780.	2.5	43
21	Engineering an N-doped Cu <sub>2</sub> O@N–C interface with long-lived photo-generated carriers for efficient photoredox catalysts. Journal of Materials Chemistry A, 2017, 5, 10220-10226.	10.3	42
22	Role of Photoinduced Exciton in the Transient Terahertz Conductivity of Few-Layer WS <sub>2</sub> Laminate. Journal of Physical Chemistry C, 2017, 121, 20451-20457.	3.1	42
23	A Water-Soluble, Green-Light Triggered, and Photo-Calibrated Nitric Oxide Donor for Biological Applications. Bioconjugate Chemistry, 2018, 29, 1194-1198.	3.6	42
24	Ultrasensitive Sensing of Volatile Organic Compounds Using a Cuâ€Doped SnO <sub>2</sub> â€NiO pâ€n Heterostructure That Shows Significant Raman Enhancement**. Angewandte Chemie - International Edition, 2021, 60, 26260-26267.	13.8	41
25	Influence of Different Diimine (N <sup>â^§</sup> N) Ligands on the Photophysics and Reverse Saturable Absorption of Heteroleptic Cationic Iridium(III) Complexes Bearing Cyclometalating 2-{3-[7-(Benzothiazol-2-yl)fluoren-2-yl]phenyl}pyridine (C <sup>â^§</sup> N) Ligands. Journal of Physical Chemistry C. 2014. 118. 23233-23246.	3.1	40
26	Ultrafast Excited-State Dynamics in Hexaethyleneglycol-Linked DNA Homoduplexes Made of A·T Base Pairs. Journal of the American Chemical Society, 2013, 135, 10290-10293.	13.7	39
27	Enhancing photo-reduction quantum efficiency using quasi-type II core/shell quantum dots. Chemical Science, 2016, 7, 4125-4133.	7.4	35
28	Excited State Decay Pathways of 2′-Deoxy-5-methylcytidine and Deoxycytidine Revisited in Solution: A Comprehensive Kinetic Study by Femtosecond Transient Absorption. Journal of Physical Chemistry B, 2018, 122, 7027-7037.	2.6	35
29	Mechanism of Photoluminescence in Ag Nanoclusters: Metal-Centered Emission versus Synergistic Effect in Ligand-Centered Emission. Journal of Physical Chemistry C, 2019, 123, 18638-18645.	3.1	33
30	Electricâ€Fieldâ€Mediated Electron Tunneling of Supramolecular Naphthalimide Nanostructures for Biomimetic H <sub>2</sub> Production. Angewandte Chemie - International Edition, 2021, 60, 1235-1243.	13.8	33
31	Shallow distance-dependent triplet energy migration mediated by endothermic charge-transfer. Nature Communications, 2021, 12, 1532.	12.8	33
32	Thymine Dimer Photoreversal in Purine-Containing Trinucleotides. Journal of Physical Chemistry B, 2012, 116, 698-704.	2.6	32
33	Sensitive determination of dopamine levels via surface-enhanced Raman scattering of Ag nanoparticle dimers. International Journal of Nanomedicine, 2018, Volume 13, 2337-2347.	6.7	29
34	Dynamic artificial light-harvesting systems based on rotaxane dendrimers. Giant, 2020, 2, 100020.	5.1	27
35	Tuning interfacial sequence between nitrogen-doped carbon layer and Au nanoparticles on metal-organic framework-derived TiO2 to enhance photocatalytic hydrogen production. Chemical Engineering Journal, 2020, 397, 125468.	12.7	26
36	Crystallization kinetics of cerium oxide nanoparticles formed by spontaneous, room-temperature hydrolysis of cerium( <scp>iv</scp> ) ammonium nitrate in light and heavy water. Physical Chemistry Chemical Physics, 2017, 19, 3523-3531.	2.8	24

#	Article	lF	CITATIONS
37	Decay Pathways of Thymine Revisited. Journal of Physical Chemistry A, 2018, 122, 4819-4828.	2.5	23
38	Ultrafast Excited-State Dynamics of Cytosine Aza-Derivative and Analogues. Journal of Physical Chemistry A, 2017, 121, 2780-2789.	2.5	22
39	A Photo-triggered and photo-calibrated nitric oxide donor: Rational design, spectral characterizations, and biological applications. Free Radical Biology and Medicine, 2018, 123, 1-7.	2.9	22
40	Reductive-damage-induced intracellular maladaptation for cancer electronic interference therapy. CheM, 2022, 8, 866-879.	11.7	21
41	Nearâ€Unity Triplet Generation Promoted via Spiroâ€Conjugation. Angewandte Chemie - International Edition, 2022, 61, .	13.8	20
42	Turn-on fluorescence detection of cysteine with glutathione protected silver nanoclusters. Methods and Applications in Fluorescence, 2019, 7, 034004.	2.3	19
43	Ultrafast Excited-State Dynamics and Vibrational Cooling of 8-Oxo-7,8-dihydro-2′-deoxyguanosine in D <sub>2</sub> O. Journal of Physical Chemistry A, 2013, 117, 12851-12857.	2.5	18
44	Using Fractional Intensities of Time-resolved Fluorescence to Sensitively Quantify NADH/NAD+ with Genetically Encoded Fluorescent Biosensors. Scientific Reports, 2017, 7, 4209.	3.3	18
45	Raman Fiber Photometry for Understanding Mitochondrial Superoxide Burst and Extracellular Calcium Ion Influx upon Acute Hypoxia in the Brain of Freely Moving Animals. Angewandte Chemie - International Edition, 2022, 61, e202111630.	13.8	18
46	Ultrafast internal conversion dynamics of bilirubin bound to UnaG and its N57A mutant. Physical Chemistry Chemical Physics, 2019, 21, 2365-2371.	2.8	17
47	A comprehensive study on the generation of reactive oxygen species in Cu-Aβ-catalyzed redox processes. Free Radical Biology and Medicine, 2019, 135, 125-131.	2.9	16
48	Photoinduced Terahertz Conductivity and Carrier Relaxation in Thermal-Reduced Multilayer Graphene Oxide Films. Journal of Physical Chemistry C, 2017, 121, 2451-2458.	3.1	15
49	Perovskite Mediated Vibronic Coupling of Semiconducting SERS for Biosensing. Advanced Functional Materials, 2022, 32, .	14.9	15
50	Ultrafast Intersystem Crossing in Epigenetic DNA Nucleoside 2′-Deoxy-5-formylcytidine. Journal of Physical Chemistry B, 2019, 123, 5782-5790.	2.6	14
51	Solventâ€Dependent Stabilization of a Charge Transfer State is the Key to Ultrafast Triplet State Formation in an Epigenetic DNA Nucleoside. Chemistry - A European Journal, 2021, 27, 10932-10940.	3.3	14
52	The phosphorescence and excitation-wavelength dependent fluorescence kinetics of large-scale graphene oxide nanosheets. RSC Advances, 2017, 7, 22684-22691.	3.6	13
53	Ultrafast Excited-State Intermolecular Proton Transfer in Indigo Oligomer. Journal of Physical Chemistry A, 2019, 123, 6463-6471.	2.5	13
54	Horizontally Aggregation of Monolayer Reduced Graphene Oxide Under Deep UV Irradiation in Solution. Nanoscale Research Letters, 2019, 14, 117.	5.7	13

#	Article	IF	CITATIONS
55	A fraction of NADH in solution is "dark― Implications for metabolic sensing via fluorescence lifetime. Chemical Physics Letters, 2019, 726, 18-21.	2.6	13
56	Direct observation of an intramolecular charge transfer state in epigenetic nucleobase <i>N</i> 6-methyladenine. Physical Chemistry Chemical Physics, 2019, 21, 6878-6885.	2.8	13
57	Sensitive Hg <sup>2+</sup> Ion Detection Using Metal Enhanced Fluorescence of Novel Polyvinyl Pyrrolidone (PVP)-Templated Gold Nanoparticles. Applied Spectroscopy, 2018, 72, 1645-1652.	2.2	12
58	Plasmonic Electronsâ€Driven Solarâ€ŧoâ€Hydrocarbon Conversion over Au NR@ZnO Coreâ€Shell Nanostructures. ChemCatChem, 2020, 12, 2989-2994.	3.7	12
59	Femtosecond Fluorescence Spectra of NADH in Solution: Ultrafast Solvation Dynamics. Journal of Physical Chemistry B, 2020, 124, 771-776.	2.6	12
60	Dithienylethene metallodendrimers with high photochromic efficiency. Chinese Chemical Letters, 2022, 33, 1613-1618.	9.0	12
61	Engineering the Chargeâ€Transfer State to Facilitate Spin–Orbit Charge Transfer Intersystem Crossing in Spirobis[anthracene]diones. Angewandte Chemie, 2020, 132, 22363-22368.	2.0	11
62	Double Insurance of Continuous Band Structure and N–C Layer Induced Prolonging of Carrier Lifetime to Enhance the Long-Wavelength Visible-Light Catalytic Activity of N-Doped In2O3. Inorganic Chemistry, 2021, 60, 1160-1171.	4.0	11
63	TPZ, a bright centrosymmetric two-photon scaffold for bioimaging. Chemical Communications, 2017, 53, 10938-10941.	4.1	10
64	Numerical Study of Novel Ratiometric Sensors Based on Plasmon–Exciton Coupling. Applied Spectroscopy, 2017, 71, 2377-2384.	2.2	9
65	Dual excited state deactivation pathways in TPZ2: A centrosymmetric dye with both high fluorescence and triplet state quantum yield. Chinese Chemical Letters, 2018, 29, 1486-1488.	9.0	9
66	Ultrafast spectroscopy of biliverdin dimethyl ester in solution: pathways of excited-state depopulation. Physical Chemistry Chemical Physics, 2020, 22, 19903-19912.	2.8	9
67	Unravelling the role of charge transfer state during ultrafast intersystem crossing in compact organic chromophores. Physical Chemistry Chemical Physics, 2021, 23, 25455-25466.	2.8	9
68	Solvent induced fluorescence enhancement of graphene oxide studied by ultrafast spectroscopy. Chemical Physics, 2018, 508, 1-6.	1.9	8
69	pH Controlled Intersystem Crossing and Singlet Oxygen Generation of 8â€Azaadenine in Aqueous Solution. ChemPhysChem, 2019, 20, 757-765.	2.1	8
70	Observation of triplet nï€* state in ultrafast intersystem crossing of 6-azathymine. Journal of Photochemistry and Photobiology A: Chemistry, 2020, 396, 112491.	3.9	8
71	Low-threshold stimulated emission in perovskite quantum dots: single-exciton optical gain induced by surface plasmon polaritons at room temperature. Journal of Materials Chemistry C, 2020, 8, 5847-5855.	5.5	8
72	New Insights about the Photostability of DNA/RNA Bases: Triplet nπ* State Leads to Effective Intersystem Crossing in Pyrimidinones. Journal of Physical Chemistry B, 2021, 125, 2042-2049.	2.6	8

#	Article	IF	CITATIONS
73	Ultrasensitive Sensing of Volatile Organic Compounds Using a Cuâ€Doped SnO <sub>2</sub> â€NiO pâ€n Heterostructure That Shows Significant Raman Enhancement**. Angewandte Chemie, 2021, 133, 26464-26471.	2.0	8
74	Dehydrogenase Binding Sites Abolish the "Dark―Fraction of NADH: Implication for Metabolic Sensing via FLIM. Journal of Physical Chemistry B, 2020, 124, 6721-6727.	2.6	7
75	Ultrafast Fluorescence Spectroscopy via Upconversion and Its Applications in Biophysics. Molecules, 2021, 26, 211.	3.8	7
76	Intramolecular Charge Transfer in 5-Halogen Cytidines Revealed by Femtosecond Time-Resolved Spectroscopy. Journal of Physical Chemistry B, 2020, 124, 2560-2567.	2.6	6
77	Regulation of Silver Nanoclusters with 4 Orders of Magnitude Variation of Fluorescence Lifetimes with Solvent-Induced Noncovalent Interaction. Journal of Physical Chemistry C, 2022, 126, 5198-5205.	3.1	6
78	Time-Resolved Fluorescence of Water-Soluble Pyridinium Salt: Sensitive Detection of the Conformational Changes of Bovine Serum Albumin. Applied Spectroscopy, 2016, 70, 1733-1738.	2.2	5
79	Direct Observation of Ultrafast Access to a Solvent-Independent Singlet–Triplet Equilibrium State in Acridone Solutions. Journal of Physical Chemistry B, 2021, 125, 13291-13297.	2.6	4
80	Mimicking Photosynthesis with Supercomplexed Lipid Nanoassemblies: Design, Performance, and Enhancement Role of Cholesterol. Langmuir, 2016, 32, 7326-7338.	3.5	3
81	Using a Fluorescent 1-Methyl-4-(2-Pyren-1-Yl-Vinyl)-Pyridinium Iodide to Characterize Solvent Polarities. Journal of Applied Spectroscopy, 2018, 84, 939-947.	0.7	3
82	Hydrogen atom and water complex determine the excited state dynamics of 8-azaguanine. Chemical Physics, 2021, 544, 111118.	1.9	3
83	The mechanodonor-acceptor coupling (MDAC) approach for unidirectional multi-state fluorochromism. Science China Chemistry, 2021, 64, 253-262.	8.2	3
84	Nearâ€Unity Triplet Generation Promoted via Spiroâ€Conjugation. Angewandte Chemie, 2022, 134, e202113190.	2.0	3
85	Raman Fiber Photometry for Understanding Mitochondrial Superoxide Burst and Extracellular Calcium Ion Influx upon Acute Hypoxia in the Brain of Freely Moving Animals. Angewandte Chemie, 0, , .	2.0	2
86	One order of magnitude increase of triplet state lifetime observed in deprotonated form selenium substituted uracil. Physical Chemistry Chemical Physics, 2022, 24, 875-882.	2.8	2
87	Excited State Dynamics of Methylated Guanosine Derivatives Revealed by Femtosecond Timeâ€resolved Spectroscopy. Photochemistry and Photobiology, 2022, 98, 1008-1016.	2.5	2
88	Fluorescence Dynamics of N-Terminal Tryptofan-X Residues in Polypeptide: pH Response. Journal of Applied Spectroscopy, 2017, 84, 633-638.	0.7	1
89	Rapid, Wide-Range, and Low-Cost Determination of Formaldehyde Based on Porous Silica Gel Plate by Digital Image Colorimetry. Proceedings (mdpi), 2019, 42, .	0.2	1
90	Near unity charge separation efficiency leads to pure ultraviolet emission in few layer graphene nanosheets. Nanotechnology, 2019, 30, 295201.	2.6	0